

Fast exciton spin relaxation in single quantum dots

I. Favero,¹ G. Cassabois,^{1,*} C. Voisin,¹ C. Delalande,¹ Ph. Roussignol,¹
R. Ferreira,¹ C. Couteau,² J. P. Poizat,² and J. M. Gérard³

¹*Laboratoire Pierre Aigrain, Ecole Normale Supérieure, 24 rue Lhomond 75231 Paris Cedex 5, France*

²*CEA-CNRS-UJF "Nanophysics and Semiconductors" Laboratory, Laboratoire de Spectrométrie Physique,
140 Avenue de la Physique - BP 87, 38402 Saint Martin d'Hères, France*

³*CEA-CNRS-UJF "Nanophysics and Semiconductors" Laboratory,
CEA/DRFMC/SP2M, 17 rue des Martyrs 38054 Grenoble Cedex 9, France*

(Dated: November 8, 2018)

Exciton spin relaxation is investigated in single epitaxially grown semiconductor quantum dots in order to test the expected spin relaxation quenching in this system. We study the polarization anisotropy of the photoluminescence signal emitted by isolated quantum dots under steady-state or pulsed non-resonant excitation. We find that the longitudinal exciton spin relaxation time is strikingly short (≤ 100 ps) even at low temperature. This result breaks down the picture of a frozen exciton spin in quantum dots.

PACS numbers: 78.67.Hc, 78.55.Cr, 78.66.Fd

Spin memory effects in semiconductor quantum dots (QDs) attract presently much attention in the physics of nanostructures. The discrete energy spectrum of zero-dimensional carriers in QDs is expected to lead to an inhibition of the main spin relaxation mechanisms which are known in bulk semiconductors and planar heterostructures [1, 2, 3]. In some novel QD devices, the preservation of the exciton spin coherence is a central issue, for instance for the generation of polarization-entangled photon-pairs in quantum information processing [4, 5]. Recent studies of epitaxially grown InGaAs/GaAs QDs have shown that the longitudinal exciton spin relaxation may be quenched over tens of ns at low temperature [6, 7, 8]. However, it was also suggested in Ref. [7] that some QDs could undergo a rapid spin relaxation, because the longitudinal spin dynamics exhibits, for QD arrays, a fast decay component (40 ps). This fact highlights the need for experiments probing spin relaxation dynamics on the single QD level. However, the implementation of the standard time-resolved techniques used for QDs ensembles [6, 7, 8] still remains an experimental challenge in the field of single QD spectroscopy.

In this letter, we report on the observation of a strikingly fast longitudinal relaxation (≤ 100 ps) of the exciton spin for some single InAs/GaAs QDs. We study single neutral QDs, isolated from a dilute QD array by micro-photoluminescence (PL). We focus our attention on QDs displaying a polarization anisotropy of their emission under non-resonant excitation. On the basis of time-resolved data and rate equation analysis, we demonstrate that this feature can only be understood as resulting from a fast direct transfer between the bright exciton states, leading to spin relaxation. This result breaks down the picture of an universal freezing of the exciton spin in QDs at low temperature.

Let us first describe the fine structure of the exciton ground state in a neutral QD, and in particular the polarization anisotropy underlying our experimental approach. Assuming rotational symmetry of the QD along

the [001] growth axis, the ground heavy-hole exciton state is fourfold degenerate with electron-hole pair states having a projection of the total angular momentum along the growth axis J_z equal to ± 1 and ± 2 . In the dipole approximation, the two $|J_z = \pm 2\rangle$ states are dark and the two $|J_z = \pm 1\rangle$ states are bright and coupled to orthogonal circularly polarized light states. The short-range part of the electron-hole exchange interaction lifts their degeneracy and the dark states lie a few hundreds of μeV below the degenerate bright states [9]. However, different microscopic effects such as the anisotropy of the QD confinement potential but also the atomistic symmetry of the crystal [10] modify this simple picture and break the QD rotational invariance. The fine structure of the exciton ground state is determined by the subtle interplay between the spin-orbit and exchange interactions as a function of the crystal atomistic symmetry and QD shape, as discussed in detail in Ref. [10]. The most important result is that the new bright states $|X\rangle$ and $|Y\rangle$ are no longer degenerate and correspond to two linearly polarized transitions which are aligned along two orthogonal principal axes of the QD. Furthermore, the symmetry reduction gives rise, through a heavy-light hole mixing [11] or through a deformation of the wave-function envelope, to different oscillator strengths γ_X and γ_Y for the bright states [12]. This phenomenon is the origin of the polarization anisotropy of the PL emission.

The observation of split linearly polarized transitions has been reported for QDs of various materials by means of single-QD spectroscopy [5, 13, 14, 15]. The ratio of the PL intensities of the $|X\rangle$ and $|Y\rangle$ states varies from one study to another and the observed polarization anisotropy is naturally interpreted in terms of different oscillator strengths for the two bright exciton states in a QD of reduced symmetry. However, to the best of our knowledge, it has never been pointed out that the observation of polarization anisotropy in PL measurements is not possible if the dynamics of the system is only driven by radiative recombination. Another relaxation mecha-

nism is needed in order to obtain different PL intensities for the $|X\rangle$ and $|Y\rangle$ lines, as explained below.

For the sake of clarity, we first analyze a three-level system with the two bright exciton states $|X\rangle$ and $|Y\rangle$ and the ground state $|g\rangle$ [Fig. 1]. We examine the results of a simple rate equation model where the QD states are equally populated with a photo-generation rate G and radiatively recombine with respective oscillator strengths γ_X and γ_Y . The fact that both bright states are equally populated is a central assumption of our model and it requires a non-resonant excitation of the QD to avoid any polarization memory of the excitation laser, as detailed below. If the system dynamics is only driven by radiative recombination [Fig. 1(a)], the steady-state PL intensity of both bright exciton states in the weak excitation regime is *exactly the same* whatever the difference in oscillator strengths. This result may be surprising at first sight but simply stems from a quantum efficiency equal to unity for both $|X\rangle$ and $|Y\rangle$ states: every single exciton which is photo-generated on a bright state will give rise to the emission of a single photon. While the steady-state populations n_X and n_Y do depend on the oscillator strengths γ_X and γ_Y ($n_\beta = G/\gamma_\beta$ with $\beta = X$ or Y), the PL intensities are only proportional to the pumping rate ($I_{|\beta\rangle} \propto \gamma_\beta n_\beta \propto G$).

This means that the polarization anisotropy observed for the QD exciton ground state in PL experiments has to be revealed by an additional relaxation channel. In the following we consider two possible schemes for this additional process: non-radiative recombination [Fig. 1(b)] and longitudinal exciton spin relaxation [Fig. 1(c)]. In both cases the PL signal exhibits a polarization anisotropy with a linear polarization ratio R_L given by:

$$R_L = \frac{I_{|X\rangle} - I_{|Y\rangle}}{I_{|X\rangle} + I_{|Y\rangle}} = \frac{\gamma_X - \gamma_Y}{\gamma_X + \gamma_Y + \gamma_X\gamma_Y/\Gamma} \quad (1)$$

where Γ is equal to $\gamma_{NR}/2$ and $\tilde{\gamma}_s$ for cases (b) and (c) of Fig. 1, respectively. In the limit of a small perturbation to the radiative recombination ($\Gamma \ll \gamma_X, \gamma_Y$) the polarization anisotropy vanishes ($R_L \sim 0$), as explained above. On the contrary, when the additional relaxation channel strongly competes with the radiative coupling ($\Gamma \gg \gamma_X, \gamma_Y$) the linear polarization ratio R_L is equal to $(\gamma_X - \gamma_Y)/(\gamma_X + \gamma_Y)$ revealing the different oscillator strengths of the bright exciton states. In fact, an efficient non-radiative recombination or spin relaxation equalizes the populations of the two bright states so that the PL intensities become proportional to their respective oscillator strengths ($I_{|\beta\rangle} \propto \gamma_\beta \tilde{n}$ where \tilde{n} is the common value of n_X and n_Y). In the following we present polarization-resolved PL experiments in single InAs/GaAs QDs which provide a clear insight into the exciton spin relaxation dynamics in isolated QDs.

Single-QD spectroscopy at low temperature is performed by standard micro-PL measurements in the far field using a microscope objective in a confocal geometry. The excitation beam is provided by a He:Ne laser and a

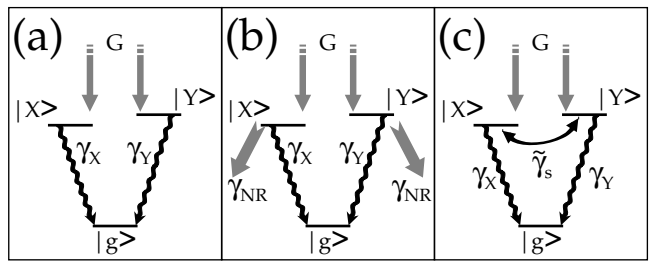


FIG. 1: Energy level diagram of a QD showing the two bright exciton states $|X\rangle$ and $|Y\rangle$ and the system ground state $|g\rangle$. (a) The system dynamics is determined by an exciton photo-generation rate G and two oscillator strengths γ_X and γ_Y accounting for radiative recombination. An additional relaxation channel is considered: non-radiative recombination (b) or longitudinal exciton spin relaxation (c).

frequency-doubled cw mode-locked Ti:Sa laser for steady-state and time-resolved PL experiments, respectively. In the steady-state PL measurements, the signal is detected, after spectral filtering by a 32 cm monochromator, by a LN₂-cooled charge-coupled-device (CCD) with a spectral resolution of 120 μeV . Life-time measurements are performed by time-correlation single photon counting with a temporal resolution of 400 ps. Polarization-resolved experiments are implemented by using a half-wave retarder and a fixed linear polarizer in front of the spectrometer in order to avoid any detection artifacts due to the anisotropic response function of the setup.

In Fig. 2 we display the polarization-resolved PL measurements under steady-state excitation, at low temperature for three types of QDs in a dilute QD array [16]. In order to better visualize the fine structure of the exciton ground state, we plot differential PL spectra $I_X - I_Y$ where we subtract the PL spectra recorded for the X and Y analysis axes, corresponding to the $[110]$ and $[\bar{1}\bar{1}0]$ crystallographic directions. In the dispersive profiles, the positive signal corresponds to the emission of the $|X\rangle$ state and the negative one to the $|Y\rangle$ state. After normalization by the PL intensity maximum of the total spectrum $I_X + I_Y$, we carefully fit our dispersive profiles with theoretical curves calculated with two orthogonal linearly polarized lines of different intensities and split by an energy Δ . Such a procedure allows us to resolve an energy splitting below the spectral resolution of our setup as shown in Fig. 2(a) ($\Delta \sim 35 \mu\text{eV}$) and (b) ($\Delta \sim 105 \mu\text{eV}$). We are nevertheless limited by the spectral extension of 45 μeV corresponding to a single CCD pixel, and also by the PL intensity asymmetry $I_{|X\rangle}:I_{|Y\rangle}$ as shown in Fig. 2(c) for a QD with $I_{|X\rangle}/I_{|Y\rangle} \sim 10$ where we only get an upper value of 40 μeV for the bright states energy splitting.

Before analyzing the dynamics of the population transfer between the bright and dark states, we would like to discuss the central assumption of our model where we consider the same exciton photo-generation rate G for both bright states. Indeed, different photo-generation

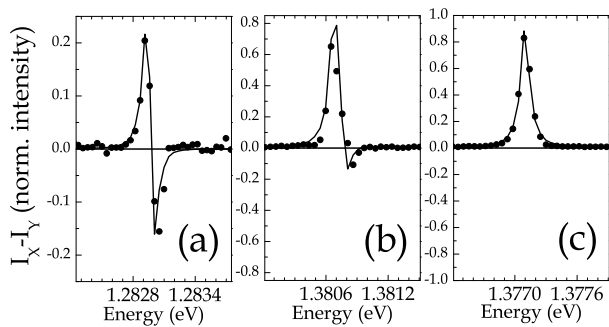


FIG. 2: Normalized differential photoluminescence spectra $I_X - I_Y$ for three quantum dots at 10K, where I_X and I_Y are the photoluminescence spectra recorded for the X and Y analysis axes, respectively. Fits (solid line) are performed with two orthogonal linearly polarized lines with $I_{|X\rangle}/I_{|Y\rangle}$ equal to 1.2 (a), 3 (b), and 10 (c), and an energy splitting $\Delta \sim 35$ μeV (a), $\Delta \sim 105$ μeV (b), and $\Delta < 40$ μeV (c).

rates G_X and G_Y for two bright exciton states of identical oscillator strengths would also lead to a polarization anisotropy. In fact, in both steady-state and time-resolved PL measurements, we perform a highly non-resonant excitation of the QDs where electron-hole pair states are photo-created in the GaAs barrier and we do not measure any modification of the linear polarization ratio R_L after rotation of the linear polarization of the excitation laser. This observation indicates that the memory of the laser polarization is lost in our experimental configuration and does not bias the carrier relaxation into the QDs. Furthermore, we rule out a differential exciton capture because, if $G_X \neq G_Y$, R_L is predicted to decrease above the QD saturation threshold in a model including multi-excitonic states [17], whereas in our power-dependent measurements R_L remains constant. We therefore validate the assumption of an identical exciton photo-generation rate G for both bright states and we now comment on our time-resolved PL experiments.

The PL decay dynamics investigated for a set of ten QDs show qualitatively the same features: (i) a bi-exponential decay of the population dynamics when the temperature increases [Fig. 3(b)] which is the signature of a coupling to the dark states [18], (ii) a constant ratio $I_{|X\rangle}(t)/I_{|Y\rangle}(t)$ of the time-resolved PL intensities of the bright states [Fig. 3(a)] whatever the temperature. Note that this latter fact implies that the time-resolved linear polarization ratio $R_L(t)$ does not exhibit any variation as a function of time.

In Fig. 3(a) we display typical time-resolved PL measurements at 5K for the X (top curve) and Y (bottom curve) polarization analysis axes. Both curves are well fitted by the numerical convolution of the temporal response function of the setup with an exponential of 450 ps time constant. The ratio $I_{|X\rangle}(t)/I_{|Y\rangle}(t)$ has thus a constant value which is *moreover the same as in steady-state*

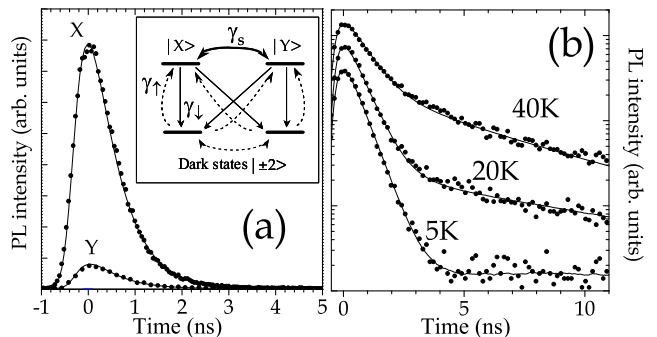


FIG. 3: (a) Time-resolved photoluminescence intensity at 5K, for the X (top curve) and Y (bottom curve) polarization analysis axes, for the QD of Fig. 2(c). (Inset): Schematic diagram of the exciton ground state fine structure. (b) Time-resolved traces for the X analysis axis at 5, 20 and 40K on a semi-logarithmic scale. Fits (solid line) are solutions of the rate equation model sketched in the inset.

measurements. Such a result is the counterpart in the temporal domain of the phenomenology discussed above in stationary conditions. Namely, in the regime where the additional relaxation channel strongly competes with the radiative coupling ($\Gamma \gg \gamma_X, \gamma_Y$), the transient populations of the bright exciton states rapidly equalize so that we monitor the global decay of the bright exciton states of different oscillator strengths ($I_{|\beta\rangle}(t) \propto \gamma_\beta \tilde{n}(t)$ where $\tilde{n}(t)$ is the common value reached by the transient exciton populations).

Let us now discuss the additional relaxation process. Non-radiative recombination is known to be negligible in InAs QDs at low temperature [19, 20]. Moreover, its efficiency is expected to increase with temperature so that the presence of non-radiative recombination centers would hasten the PL decay when rising the temperature. On the contrary, an overall slow-down of the carrier dynamics is observed in our experiments [Fig. 3(b)] with a bi-exponential decay of the PL dynamics due to the exciton dark states [18]. We therefore conclude that non-radiative recombination does not play a major role in the bright states recombination [Fig. 1(b)] and that a fast exciton spin relaxation occurs in our single QDs [Fig. 1(c)].

In order to get quantitative information on the exciton spin relaxation, we generalize the model of Fig. 1(c) by taking into account the dark exciton states which lead to the bi-exponential decay of the population dynamics [Fig. 3(b)]. Extending the approach of Labeau *et al.* [18], we use a five-level system and we calculate the population dynamics according to the model sketched in the inset of Fig. 3. The population relaxation rate from a bright to a dark state is γ_0 at zero temperature. We account for an acoustic phonon-assisted thermalization with a rate $\gamma_\downarrow = \gamma_0(N + 1)$ for each bright-to-dark chan-

nel and $\gamma_{\uparrow} = \gamma_0 N$ for each dark-to-bright one, where $N = 1/[\exp(\Omega/k_B T) - 1]$ is the Bose-Einstein phonon number and Ω is the energy splitting between the bright and dark states, which lifetime is $1/\gamma_D$. For the population relaxation among the bright states, we take the same transfer rate γ_s for both paths because $\Delta \ll k_B T$. This model yields, for the steady-state linear polarization ratio R_L , the expression given in Eq. 1 where the effective spin relaxation rate $\tilde{\gamma}_s$ introduced in Fig. 1(c) is equal to $\gamma_s + \gamma_{\downarrow}$. As far as the time-resolved experiments are concerned, we assume that the bright and dark states are equally populated at $t=0$ and we plot in solid lines in Fig. 3(a) and (b) the solutions of our rate equation model after numerical convolution with the temporal response function of the setup. We observe a fair agreement with all our time-resolved measurements, for realistic values of $1/\gamma_D \sim 8.5$ ns and $\Omega \sim 250$ μ eV [9].

The efficient direct population transfer between the $|X\rangle$ and $|Y\rangle$ states is the origin of the constant ratio $I_{|X\rangle}(t)/I_{|Y\rangle}(t)$ of the time-resolved PL intensities [Fig. 3(a)], and we find that the corresponding time constant is smaller than 100 ps ($1/\gamma_s \leq 0.1$ ns). At low temperature (5K) the influence of the dark states on the exciton dynamics is only marginal. The quasi-exponential dynamics of the global population of the bright states has a decay time τ corresponding to the oscillator strengths average $(1/\tau \sim (\gamma_X + \gamma_Y)/2)$. Given the oscillator strengths ratio $\gamma_X/\gamma_Y \sim I_{|X\rangle}(t)/I_{|Y\rangle}(t) \sim 10$, we obtain radiative lifetimes $1/\gamma_X \sim 0.24$ ns and $1/\gamma_Y \sim 2.4$ ns. Indeed, since spin relaxation is faster than radiative recombination, we do not observe the separate decays of the bright states populations but their global common relaxation. If we decrease the population transfer rate γ_s in our simulations, we obtain distinct dynamics for the transient populations $n_X(t)$ and $n_Y(t)$ as well as a decrease of the steady-state value of the linear polarization ratio R_L , in contradiction to our experimental findings. Such an efficient exciton spin relaxation is a very important and unexpected conclusion of our study that applies to all QDs showing any detectable polarization anisotropy in their PL emission under non-resonant excitation. Complementary measurements (to be reported elsewhere) show that the breakdown of the frozen exciton spin picture can also be observed in QDs ensembles with a weak polarization anisotropy. The striking fast exci-

ton spin relaxation in neutral QDs raises fundamental theoretical questions on the corresponding microscopic mechanisms, which are beyond the scope of this work.

We finally discuss whether the indirect channel opened by the coupling to the dark states can also result in an efficient population transfer between the bright states. The relaxation rates to the dark states are determined from the analysis of the temperature-dependent data [Fig. 3(b)]. When the temperature increases, the gradual thermalization of the bright and dark states populations gives rise to the bi-exponential decay where the slow component decay time is related to the dark state lifetime. Note that a complete thermalization would lead to a quasi-exponential PL decay determined by the global dynamics of the bright and dark states. From our temperature-dependent data, we deduce a zero-temperature relaxation time $1/\gamma_0 \sim 440$ ns. For this QD, the relaxation to the dark states plays a minor role compared to the direct population transfer between bright excitons. On the other hand, for another QD (not shown) we have measured a zero-temperature relaxation time as small as $1/\gamma_0 \sim 30$ ns which is one order of magnitude shorter than above. The corresponding effective spin relaxation is $1/\gamma_{\downarrow} \sim 13$ ns at 5K and 2 ns at 40K. This results demonstrates that the population redistribution via the dark states remains anyway negligible for this QD compared to the direct transfer between the bright states ($\gamma_{\downarrow} \ll \gamma_s$ in $\tilde{\gamma}_s = \gamma_s + \gamma_{\downarrow}$).

In summary, we have studied the longitudinal exciton spin relaxation dynamics in single QDs by analyzing the population transfer between the bright and dark states forming the exciton fine structure in neutral InAs quantum dots. We find that the longitudinal exciton spin relaxation time is strikingly short (≤ 100 ps) even at low temperature. This result breaks down the picture of an universal freezing of the exciton spin for QDs at low temperature. Further work is clearly needed to elucidate the interplay between the fine structure and the exciton spin relaxation, and to determine the experimental parameters that control the efficiency of spin relaxation.

LPA-ENS is "unité mixte (UMR 8551) de l'ENS, du CNRS, des Universités Paris 6 et 7". This work is financially supported by the ACI "Polqua", and by the region Ile de France through the project SESAME E-1751.

*Electronic address: Guillaume.Cassabois@lpa.ens.fr

-
- [1] *Optical orientation*, edited by F. Meier and B. Zakharchenya, Modern Problems in Condensed Matter Sciences Vol. 8, (North-Holland, Amsterdam, 1984).
 - [2] M. Z. Maialle *et al.*, Phys. Rev. B **47**, 15776 (1993).
 - [3] A. V. Khaetskii *et al.*, Phys. Rev. B **61**, 12639 (2000).
 - [4] E. Moreau *et al.*, Phys. Rev. Lett. **87**, 183601 (2001).
 - [5] C. Santori *et al.*, Phys. Rev. B **66**, 045308 (2002).
 - [6] M. Paillard *et al.*, Phys. Rev. Lett. **86**, 1634 (2001).
 - [7] A. S. Lenihan *et al.*, Phys. Rev. Lett. **88**, 223601 (2002).
 - [8] W. Langbein *et al.*, Phys. Rev. B **70**, 033301 (2004).
 - [9] M. Bayer *et al.*, Phys. Rev. B **65**, 195315 (2002).
 - [10] G. Bester *et al.*, Phys. Rev. B **67**, 161306 (2003).
 - [11] T. Tanaka *et al.*, Appl. Phys. Lett. **62**, 756 (1993).
 - [12] L. W. Wang *et al.*, Phys. Rev. B **59**, 5678 (1999).
 - [13] D. Gammon *et al.*, and D. Park, Phys. Rev. Lett. **76**, 3005 (1996).
 - [14] M. Bayer *et al.*, Phys. Rev. Lett. **82**, 1748 (1999).
 - [15] L. Besombes *et al.*, Phys. Rev. Lett. **85**, 425 (2000).
 - [16] for a sample description and a systematic study of the polarization anisotropy, see I. Favero *et al.*, Appl. Phys.

- Lett. **86**, 041904 (2005).
- [17] E. Dekel *et al.*, Phys. Rev. B **62**, 11038 (2000).
- [18] O. Labeau *et al.*, Phys. Rev. Lett. **90**, 257404 (2003).
- [19] J. M. Gérard *et al.*, Appl. Phys. Lett. **68**, 3123 (1996).
- [20] I. Robert *et al.*, Physica E **13**, 606 (2002).